Analyst

RSC Publishing

PAPER

View Article Online
View Journal

Aptamer-linked biosensor for thrombin based on AuNPs/thionine–graphene nanocomposite

Cite this: DOI: 10.1039/c3an01006f

Zhao Zhang,[a] Liqiang Luo,*[a] Limei Zhu,[a] Yaping Ding,[a] Dongmei Deng[a] and Zhenxin Wang*[b]

A novel protocol of electrochemical thrombin aptasensor based on a gold nanoparticles/thionine–graphene (AuNPs/Th–G) nanocomposite modified glassy carbon electrode was presented. Graphene was non-covalently functionalized by thionine *via* π-stacking interaction, and then AuNPs were electrodeposited onto the Th–G surface. The morphology and conductivity of the AuNPs/Th–G nanocomposite were characterized by scanning electron microscopy, cyclic voltammetry and electrochemical impedance spectroscopy. The ethanethiol-substituted oligonucleotide probe was immobilized onto the surface of the AuNPs/Th–G nanocomposite to prepare an electrochemical biosensing platform. The aptamer–thrombin reaction was monitored by differential pulse voltammetry. Under optimum conditions, the proposed biosensor exhibits high sensitivity and a low detection limit for thrombin determination. The thrombin could be quantified in a wide range of 0.5 to 40 nM and with a low detection limit of 0.093 nM ($S/N = 3$).

Received 20th May 2013
Accepted 19th June 2013

DOI: 10.1039/c3an01006f

www.rsc.org/analyst

1 Introduction

Aptamers, screened through the systematic evolution of ligands by exponential enrichment process from random RNA or DNA libraries, are artificial oligonucleic acids or peptide molecules that bind to specific target molecules, such as small molecules, proteins, nucleic acids, and even cells, tissues and organisms.[1,2] As recognition elements, aptamers have potential applications in basic research and clinical applications.[3,4] To date, thrombin aptamers have been extensively investigated because of the important role of thrombin in thrombosis and haemostasis. Various techniques including electrochemistry,[5–7] fluorescence,[8] surface enhanced Raman spectroscopy,[9] surface plasmon resonance[10] and quartz crystal microbalance[11] have been developed for thrombin aptasensors. Among them, electrochemical techniques have received considerable attention due to its advantages of low cost, high sensitivity, selectivity and inherent miniaturization.[12]

Gold nanoparticles (AuNPs) are a kind of well-known bionanomaterial with unique properties of large specific surface area, essential nontoxicity, excellent biocompatibility and ease of functionalization with a variety of ligands.[13,14] Due to these unique properties, AuNPs have been utilized as intermediators to immobilize biomolecules onto sensitive biosensing platforms and have shown wide application prospects in constructing electrochemical sensors covering DNA–AuNPs assemblies,[15,16] enzymes biosensors[17–19] and immunosensors.[20–22] Tang *et al.*[16] have proposed a novel electrochemical biosensor based on the self-assembly of AuNPs onto the mercaptophenyl film for DNA determination. Cui and Li[19] have constructed a label-free electrochemiluminescence (ECL) aptasensor for the sensitive and selective detection of thrombin by target-induced direct ECL signal change based on luminol functionalized AuNPs platform. Yu *et al.*[20] have developed a label-free electrochemical immunosensor based on the combination of AuNPs and mediated charge transport through multilayer films for the detection of protein analytes without redox-active centers.

Graphene, isolated by mechanically peeling off graphite crystals in 2004,[23,24] has become one of the most exciting topics of research in recent years. The two-dimensional single-atom-thick carbon material has exhibited unique properties such as low manufacturing cost,[25] high specific surface area, rapid heterogeneous electron transfer[26,27] and great mechanical strength.[28] Thanks to its biocompatibility, graphene has been employed as an excellent substrate in the detection of various target DNA sequences and proteins.[29–31] Li *et al.*[29] have reported a highly sensitive and selective sandwich structure DNA electrochemical sensor based on the ssDNA self-assembling onto a graphene surface by base-π stacking interactions. Gan *et al.*[30] have developed a label-free sensitive thrombin aptasensor with nafion–graphene nanocomposite by monitoring the current change of methylene blue immobilized on the biosensing platform. Yang *et al.*[31] have constructed a nanocomposite by grafting aptamers on graphene for a label-free thrombin biosensor with good selectivity, low detection limit and high sensitivity.

[a]*College of Sciences, Shanghai University, Shanghai 200444, PR China. E-mail: luck@shu.edu.cn; Tel: +86 21 66134734*

[b]*State Key Laboratory of Electroanalytical Chemistry, Changchun Institute of Applied Chemistry, Chinese Academy of Sciences, Changchun 130022, PR China. E-mail: wangzx@ciac.jl.cn; Tel: +86 431 85262243*

In this work, a novel electrochemical aptasensor based on AuNPs/thionine–graphene (AuNPs/Th–G) nanocomposite was fabricated for thrombin determination by differential pulse voltammetry (DPV). Graphene provided an electronically low-noise biosensing platform, and the functionalization of graphene by thionine improved its stability and preserved its intrinsic properties such as high specific surface area, good electrical conductivity and biocompatibility. Meanwhile, thionine performed as an electrochemical redox probe in DPV detection of the electrochemical aptasensor. AuNPs were electrodeposited on the Th–G surface for site-specific attachment of the thiolated thrombin-binding aptamer (TBA) based on gold–thiol chemistry. Thrombin molecules were caught by TBA and thus restrained the electron transfer to the electrode surface, resulting in a decrease of thionine DPV signal. According to the changes in DPV signal before and after thrombin recognition, trace detection of thrombin could be achieved.

2 Experimental

2.1 Reagents

Thrombin (2000 U) was purchased from Shanghai Source Leaf Biological Tech Co., Ltd. Graphite oxide (GO) was obtained from Nanjing XFNANO Materials Tech Co., Ltd. (Nanjing, China). Hydrazine hydrate ($NH_2NH_2 \cdot H_2O$, 80%) was purchased from Aladdin Co., Ltd. (Shanghai, China). Thionine was provided by Sigma Co. (USA). Bovine serum albumin (BSA), $HAuCl_4 \cdot 4H_2O$, KH_2PO_4, $K_2HPO_4 \cdot 3H_2O$, NaCl, $K_3Fe(CN)_6$ and $K_4Fe(CN)_6 \cdot 3H_2O$ were provided by Sinopharm Chemical Reagent Beijing Co., Ltd. The synthetic oligonucleotide ssDNA (TBA, 5′–SH–$(CH_2)_6$-GGT TGG TGT GGT TGG-3′)[32] was provided by Sangon Biotech Co., Ltd. (Shanghai, China). 2 μM TBA stock solution was prepared in 50 mM Tris–HCl/0.1 M NaCl/0.2 M KCl/5 mM $MgCl_2$ (pH 7.0) buffer.

2.2 Instruments and characterization

Scanning electron microscopy (SEM) images were carried out on an XL30 ESEM-FEG (Netherlands, FEI Company, at an acceleration voltage of 20.0 kV). DPV and cyclic voltammetry (CV) measurements were performed on a CHI 660D electrochemical workstation (Shanghai CH Instrument Co., China). A conventional three-electrode system was used with a saturated calomel electrode (SCE) as the reference electrode, a platinum sheet as the counter electrode and a modified glassy carbon electrode (GCE, $\Phi = 3$ mm) as the working electrode. DPV scanning potential was from −0.6 V to +0.2 V with the amplitude of 5 mV s^{-1}. Electrochemical impedance spectroscopy (EIS) measurements were tested by a Solartron 1255B Frequency Response Analyzer/SI 1287 Electrochemical Interface (Scribner Associates, Inc.) using 10 mM $[Fe(CN)_6]^{3-/4-}$ as the electrochemical probe. 5 mV amplitude of sine voltage signal was applied under open circuit potential and the frequency varied from 0.1 Hz to 100 kHz.

2.3 Preparation of the Th–G nanocomposite

The Th–G nanocomposite was prepared according to the literature.[33] Briefly, 5 mg GO was dispersed in 50 mL water, and the dispersion was exfoliated by sonicating at room temperature for 40 min. The GO dispersion was centrifuged at 3000 rpm for 5 min to obtain claybank supernatant. Then, 10 mL of 2 mM aqueous thionine was added, and the mixture was stirred vigorously for 12 h. After that, 200 μL $NH_2NH_2 \cdot H_2O$ (80%) was dropped into the above solution. The obtained mixture was vigorously shaken for 10 min and heated to 95 °C for 1 h under reflux. Then, the stable dark dispersion was centrifuged and washed three times. Finally, the products (Th–G) were dried in a vacuum oven at 80 °C for 3 h and then collected for further use.

2.4 Fabrication of aptasensor and electrochemical determination

Prior to surface modification, the GCE was polished carefully with 1.0, 0.3 and 0.05 μm alumina powder, respectively. The polished GCE was cleaned sequentially with 1 : 1 HNO_3, ethanol and water with continuously sonicating for 3 min, respectively. Then, the electrode was allowed to dry at ambient temperature. 5 μL of 1 mg mL^{-1} Th–G was dropped onto the surface of GCE and allowed to air dry to form Th–G/GCE. Subsequently, the Th–G/GCE was immersed in 0.1 M KNO_3 solution +0.2 g L^{-1} $HAuCl_4$ to electro-deposit AuNPs by cyclic sweeping between −0.5 V and 0 V at 100 mV s^{-1} for 30 cycles.[34] The obtained Au/Th–G/GCE was rinsed with deionized water and dried under an N_2 stream. After that, 20 μL of 2 μM TBA was dropped on the surface of the Au/Th–G/GCE and incubated for 12 h at room temperature in 100% humidity. Finally, the TBA/Au/Th–G/GCE was rinsed carefully with buffer, dried under an N_2 stream and stored at 4 °C for further use.

The desired concentration of thrombin solution (20 μL) was deposited on the surface of TBA/Au/Th–G/GCE and kept for 40 min at 35 °C. Then, the above electrode was rinsed with 0.1 M PBS + 0.01 M NaCl (pH 7.0) to remove the non-binding thrombin. A schematic representation of the aptasensor is displayed in Fig. 1.

3 Results and discussion

3.1 Characterization of the Th–G and Au/Th–G nanocomposite

The morphologies of the as-prepared Th–G and Au/Th–G nanocomposite were characterized by SEM. Fig. 2A reveals that Th–G is single flake. The well-exfoliated Th–G provided an ideal matrix for the distribution of AuNPs. As shown in Fig. 2B, a layer

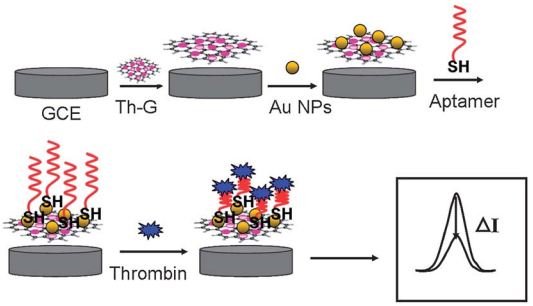

Fig. 1 Schematic diagram of the thrombin aptasensor.

of uniform AuNPs with the size of around 100 nm in diameter were dispersed on Th–G surface after electro-deposition. The AuNP layer not only increases the electrochemically activated surface area of the electrode but also provides a specific surface for TBA immobilization.[14]

3.2 Characterization of different electrodes

Fig. 3 shows the CVs and the Nyquist diagrams of 10 mM $[Fe(CN)_6]^{3-/4-}$ (1 : 1) at different electrodes. As shown in Fig. 3A, the peak current of $[Fe(CN)_6]^{3-/4-}$ at Th–G/GCE (curve b) was larger than that at bare GCE, and the electrochemical redox reversibility of $[Fe(CN)_6]^{3-/4-}$ at Th–G/GCE was better than that at bare GCE. The experimental result shows that Th–G nanocomposite has been successfully fixed on the surface of the GCE. When AuNPs were deposited on Th–G/GCE, the electrical conductivity of Au/Th–G/GCE (curve c) was enhanced further. After TBA was assembled to Au/Th–G/GCE, the peak current of $[Fe(CN)_6]^{3-/4-}$ at TBA/Au/Th–G/GCE (curve d) became much smaller than that at Au/Th–G/GCE, proving that TBA has been fixed successfully on Au/Th–G/GCE. This was due to that the negative charge of phosphoric acid groups on the aptamer interfering with the diffusion of $[Fe(CN)_6]^{3-/4-}$ to the electrode surface.[35,36] After incubation with thrombin, the formation of the aptamer–thrombin complex on the modified electrode surface resulted in a further decrease of current value (curve e) because the insulating layer of protein molecules significantly hindered the interfacial electron transfer to the modified electrode surface.[37,38]

EIS has been proved to be a powerful tool for investigating the interfacial properties of biorecognition events coupled with a graphene platform.[39] In EIS, the semicircle portion observed at high frequencies corresponds to the electron transfer limiting process, while the linear part at lower frequencies relates to diffusion processes. Fig. 3B is the Nyquist diagram of different modified electrodes. As shown in Fig. 3B, the interfacial electron transfer resistance (R_{et}) value of Th–G/GCE decreased from 135.6 Ω (curve b) to 47.9 Ω (curve a), indicating that Th–G had good electrical conductivity. This was because the electron transfer interaction to the electrode surface was promoted by electrostatic interaction between the positively charged NH_3^+ on Th–G and the negatively charged $[Fe(CN)_6]^{3-/4-}$. After AuNPs were deposited, the observed R_{et} value of Au/Th–G/GCE was much smaller (24 Ω, curve c). When TBA was immobilized on Au/Th–G/GCE, the R_{et} value of TBA/Au/Th–G/GCE increased to 1252 Ω (curve d). After the reaction between thrombin and TBA, the R_{et} value of thrombin/TBA/Au/Th–G/GCE increased to 1707 Ω (curve e). The EIS results are consistent with those of the CVs in Fig. 3A.

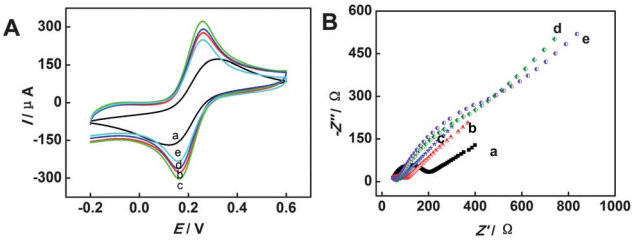

Fig. 3 CVs (A) and EISs (B) of bare GCE (a), Th–G/GCE (b), Au/Th–G/GCE (c), TBA/Au/Th–G/GCE (d) and 20 nM thrombin/TBA/Au/Th–G/GCE (e) in 0.1 M PBS (pH 7.0) containing 10 mM $[Fe(CN)_6]^{3-/4-}$ (1 : 1). The scan rate is 100 mV s^{-1} in the CV graph. The frequency varied from 0.1 Hz to 100 kHz and 5 mV amplitude of sine voltage signal was used in the EIS graph.

Thionine is a small planar molecule and contains one heterocyclic nitrogen atom and two amine groups symmetrically distributed on each side. Due to its good electroactivity, thionine has been widely utilized as a functional unit in electrochemical biosensors.[40,41] Here, thionine was used to noncovalently functionalize graphene because its planar aromatic structure could strongly interact with the graphene surface through π-stacking force.[42] CV was employed to investigate the redox peak signals of thionine at different modified electrodes. As shown in Fig. 4, a couple of well-defined redox peaks of thionine were observed (curve a) at Th–G/GCE, indicating that thionine on graphene retained its redox properties.[43] In addition, the peak currents of thionine at different electrodes decreased in the following order: Au/Th–G/GCE (curve b) > TBA/Au/Th–G/GCE (curve c) > thrombin/TBA/Au/Th–G/GCE (curve d). The CV results demonstrated that thionine could perform as an electrochemical redox probe for detecting thrombin using our electrochemical aptasensor.

Fig. 5 shows CVs of TBA/Au/Th–G/GCE in 0.1 M PBS at different scanning rates. In the scan rate range of 10 to 300 mV s^{-1}, both anodic peak current and cathodic peak current of TBA/Au/Th–G/GCE increased linearly, indicating that electron

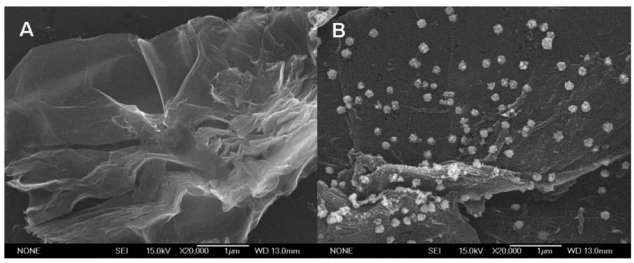

Fig. 2 SEM images of Th–G (A) and Au/Th–G (B).

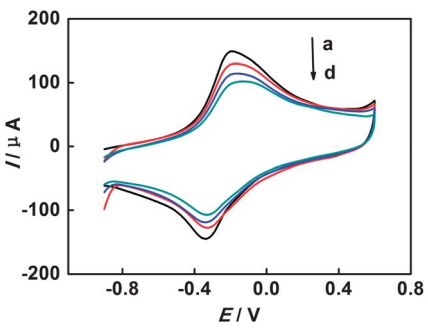

Fig. 4 CVs of the Th–G/GCE (a), Au/Th–G/GCE (b), TBA/Au/Th–G/GCE (c) and 20 nM thrombin/TBA/Au/Th–G/GCE (d) in 0.1 M PBS (pH 7.0).

transfer on the modified electrode was a surface-controlled electrochemical process.

3.3 Optimization of the sensing conditions

As mentioned above, due to the good electrochemical redox properties, thionine can serve as an electrochemical redox probe in the electrochemical aptasensor. After aptamer–thrombin reaction on TBA/Au/Th–G/GCE, an insulation layer of protein formed, obstructing electron transfer to the electrode surface. Therefore, the electrochemical oxidation peak current of thionine decreased with the increasing concentration of thrombin. The difference between the DPV current intensity (ΔI) of TBA/Au/Th–G/GCE and that of thrombin/TBA/Au/Th–G/GCE was adopted to quantitatively detect thrombin, *i.e.*, ($\Delta I = I_{\mathrm{TBA}} - I_{\mathrm{thrombin}}$).

Factors (*e.g.*, pH value, reaction temperature and reaction time) affecting the aptasensor sensing performance were studied systematically. Fig. 6A shows the effect of pH values on the value of ΔI. ΔI increased with the increasing pH value from 6.6 to 7.0, and then decreased when pH was higher than 7.0. So, pH 7.0 was chosen as the optimal pH value. Because the highest ΔI value was obtained at 35 °C, the aptamer–thrombin reaction was performed at 35 °C in the study (as shown in Fig. 6B). In addition, the ΔI was also affected by the aptamer–thrombin reaction time, the peak value of ΔI was obtained at 40 min (as shown in Fig. 6C). Therefore, 40 min was selected as the optimized reaction time in further experiments.

3.4 Determination of thrombin

Under optimized conditions, the measurement signal (ΔI) increased linearly with concentration of thrombin from 0.5 to 40 nM (ΔI (μA) = 1.0096 + 0.8097C (nM) with a correlation coefficient of 0.9953, as shown in Fig. 7). A detection limit of 0.093 nM was achieved ($S/N = 3$). The experimental result indicates that our proposed aptasensor has excellent sensitivity and a relatively wide dynamic range, as shown in Table 1.

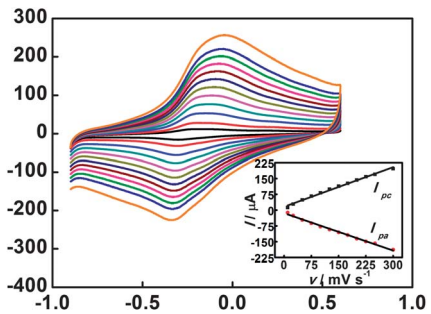

Fig. 5 CVs of TBA/Au/Th–G/GCE in 0.1 M PBS (pH 7.0) at scan rates of 10, 25, 50, 75, 100, 125, 150, 175, 200, 250 and 300 mV s^{-1}. Inset shows the plots of redox peak current *vs.* scan rate.

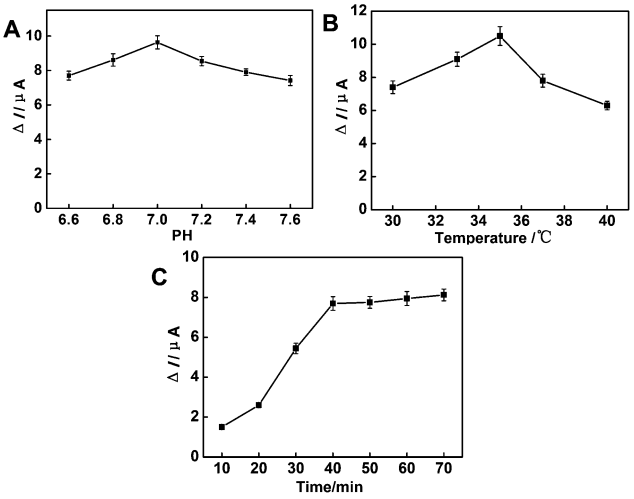

Fig. 6 Optimization of TBA/Au/Th–G/GCE sensing conditions. pH value (A): 6.6, 6.8, 7.0, 7.2, 7.4 and 7.6; aptamer–thrombin reaction temperature (B): 30, 33, 35, 37 and 40 °C; aptamer–thrombin reaction time (C): 10, 20, 30, 40, 50, 60 and 70 min, respectively.

3.5 Interference study

Fig. 8 shows DPV graphs of TBA/Au/Th–G/GCE in the presence of 10 nM thrombin (curve a), 1 mM BSA + 1 mM lysozyme sample (curve b), 10 nM thrombin + 1 mM BSA + 1 mM lysozyme sample (curve c) and 0 nM thrombin (curve d), respectively. The foreign substances caused an approximately ±6.5% relative error in the determination. The results show that the foreign substances did not interfere significantly with thrombin determination. Namely, the as-prepared TBA/Au/Th–G/GCE has excellent selectivity, which could be used to detect thrombin in practical samples.

3.6 Reproducibility and stability

To evaluate the reproducibility, four trials were run using TBA/Au/Th–G/GCE from several batches, which were prepared on different days. A satisfying relative standard deviation (R.S.D.) of 3.86% ($n = 4$) was estimated, showing that the electrochemical aptasensor has good reproducibility. After the aptasensor was stored in the refrigerator for two weeks, the peak current intensity of TBA/Au/Th–G/GCE retained 85.3% of the original value, revealing that the aptasensor has excellent stability.

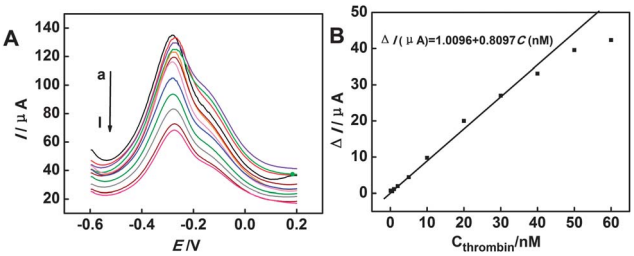

Fig. 7 (A): DPVs of TBA/Au/Th–G/GCE reacting with different concentrations of thrombin: 0, 0.1, 0.5, 1, 2, 5, 10, 20, 30, 40, 50 and 60 nM (a → l) in 0.1 M PBS (pH 7.0). (B): Plot of ΔI *vs.* C_{thrombin}.

Table 1 Performance comparison of different sensors

Detection technology	Modifier	Redox probe	Linear range (nM)	Detection limit (nM)	Ref.
DPV	Nafion@graphene	Methylene blue	0.01–50	0.006	30
DPV	Nanogold–chitosan composite	Methylene blue	1–60	0.5	45
DPV	DNA/DNA duplex	Methylene blue	6–60	3	46
DPV	Aptamer self-assembly	Ferrocene	0–10	0	47
DPV	Aptamer self-assembly	Ferrocene	5–35	0.5	48
EIS	AuNPs	$[Fe(CN)_6]^{3-/4-}$	0.1–30	0.013	49
EIS	GNPs	$[Fe(CN)_6]^{3-/4-}$	0.12–30	0.03	50
DPV	AuNP/Th–G	Thionine	0.5–40	0.093	This work

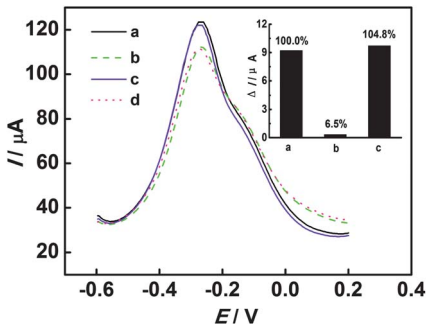

Fig. 8 DPVs of TBA/Au/Th–G/GCE reacting with 10 nM thrombin (a), 1 mM BSA + 1 mM lysoenyme (b), 10 nM thrombin + 1 mM BSA + 1 mM lysoenyme (c), 0 nM thrombin (d) in 0.1 M PBS (pH 7.0).

3.7 Determination of thrombin in human blood serum samples

In order to prove the application feasibility of the aptasensor in practical samples, the sensor was applied to determine thrombin in human blood serum samples under optimal experimental conditions. Serum is what remains from whole blood after coagulation and healthy people's serum doesn't contain thrombin.[44] In this case, the serum sample of healthy man was diluted 10 times with 0.1 M PBS (pH 7.0). As shown in Fig. 9, in the presence of 10 nM thrombin, the peak current intensity of TBA/Au/Th–G/GCE in human serum is as high as that of TBA/Au/Th–G/GCE in 0.1 M PBS. The aforementioned results show that the as-prepared aptasensor has potential application in complex biological samples.

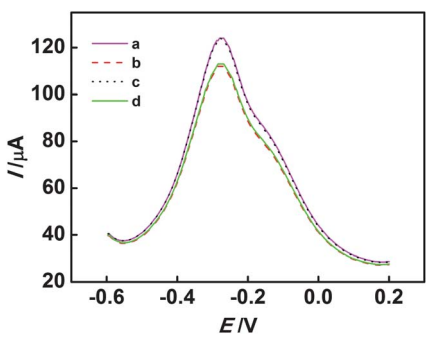

Fig. 9 DPVs of TBA/Au/Th–G/GCE reacting with 0 nM thrombin (a), 10 nM thrombin (b), 0 nM thrombin + serum (c) and 10 nM thrombin + serum (d) in 0.1 M PBS (pH 7.0).

4 Conclusion

An electrochemical aptasensor based on AuNPs/Th–G nanocomposite has been developed for quantitative determination of thrombin with high sensitivity and selectivity. In our approach, AuNPs/Th–G nanocomposite provides abundant binding sites for the immobilization of TBA on the GCE surface due to the large surface area of the AuNPs/Th–G nanocomposite. The detection of thrombin is achieved by monitoring the change of ΔI, which is caused by the aptamer–thrombin reaction. The aptasensor has a wide detection range and a low detection limit under optimal conditions. Furthermore, the proposed aptasensor shows potential for detecting specific protein species in practical samples.

Acknowledgements

The authors would like to thank the National Science Foundation of China (no. 21271127, 61171033), the NanoFoundation of Science and Techniques Commission of Shanghai Municipality (no. 12nm0504200), and the Leading Academic Discipline Project of Shanghai Municipal Education Commission (J50102) for financial support.

References

1 C. Tuerk and L. Gold, *Science*, 1990, **249**, 505–510.
2 A. D. Ellington and J. Szostak, *Nature*, 1990, **346**, 818–822.
3 T. Hianik and J. Wang, *Electroanalysis*, 2009, **21**, 1223–1235.
4 G. Z. Zhu, M. Ye, M. J. Donovan, E. Q. Song, Z. L. Zhao and W. H. Tan, *Chem. Commun.*, 2012, **48**, 10472–10480.
5 F. L. Floch, H. A. Ho and M. Leclerc, *Anal. Chem.*, 2006, **78**, 4727–4731.
6 Y. C. Huang, B. X. Ge, D. Sen and H. Z. Yu, *J. Am. Chem. Soc.*, 2008, **130**, 8023–8039.
7 X. Y. Wang, P. Dong, W. Yun, Y. Xu, P. G. He and Y. Z. Fang, *Biosens. Bioelectron.*, 2009, **24**, 3288–3292.
8 J. H. Liu, J. S. Li, Y. Jiang, S. Yang, W. H. Tan and R. H. Yang, *Chem. Commun.*, 2011, **47**, 11321–11323.
9 H. S. Cho, B. R. Baker, C. V. Pagba, T. A. Laurence, S. M. Lane and L. P. Lee, *Nano Lett.*, 2008, **8**, 4386–4390.

10 L. Wang, C. Z. Zhu, L. Han, L. H. Jin, M. Zhou and S. J. Dong, *Chem. Commun.*, 2011, **47**, 7794–7796.
11 Q. Chen, W. Tang, D. Z. Wang, X. J. Wu, N. Li and F. Liu, *Biosens. Bioelectron.*, 2010, **26**, 575–579.
12 L. P. Jiang, R. Yuan, Y. Q. Chai, Y. L. Yuan, L. J. Bai and Y. Wang, *Analyst*, 2012, **137**, 2415–2420.
13 Y. Li, C. Jing, L. Zhang and Y. T. Long, *Chem. Soc. Rev.*, 2012, **41**, 632–642.
14 N. M. Adams, S. R. Jackson, F. R. Haselton and D. W. Wright, *Langmuir*, 2012, **28**, 1068–1082.
15 T. Chinnasamy, K. Senthilkumar, A. Periyakaruppan, J. S. Devakirubakaran and A. Muthukaruppan, *Anal. Biochem.*, 2011, **417**, 73–79.
16 F. Li, Y. Feng, P. J. Dong, L. M. Yang and B. Tang, *Biosens. Bioelectron.*, 2011, **26**, 1947–1952.
17 A. Gole, C. Dash, C. Soman, S. R. Sainkar, M. Rao and M. Sastry, *Bioconjugate Chem.*, 2001, **12**, 684–690.
18 J. Zhang, P. P. Chen, X. Y. Wu, J. H. Chen, L. J. Xu, G. N. Chen and F. F. Fu, *Biosens. Bioelectron.*, 2011, **26**, 2645–2650.
19 F. Li and H. Cui, *Biosens. Bioelectron.*, 2013, **39**, 261–267.
20 C. R. Chen, D. Y. Liu, Z. S. Wu, Q. M. Luo, G. L. Shen and R. Q. Yu, *Electrochem. Commun.*, 2009, **11**, 1869–1872.
21 K. J. Huang, D. J. Niu, J. Y. Sun and J. J. Zhu, *J. Electroanal. Chem.*, 2011, **656**, 72–77.
22 C. F. Ding, F. Zhao, R. Ren and J. M. Lin, *Talanta*, 2009, **78**, 1148–1154.
23 K. S. Novoselov, A. K. Geim, S. V. Morozov, D. Jiang, Y. Zhang, S. V. Dubonos, I. V. Grigorieva and A. A. Firsov, *Science*, 2004, **306**, 666–669.
24 J. C. Meyer, A. K. Geim, M. I. Katsnelson, K. S. Novoselov, T. J. Booth and S. Roth, *Nature*, 2007, **446**, 60–63.
25 M. Segal, *Nat. Nanotechnol.*, 2009, **4**, 612–614.
26 M. Pumera, *Chem. Soc. Rev.*, 2010, **39**, 4146–4157.
27 L. A. L. Tang, J. Wang and K. P. Loh, *J. Am. Chem. Soc.*, 2010, **132**, 10976–10977.
28 X. Zhao, Q. H. Zhang and D. J. Chen, *Macromolecules*, 2010, **43**, 2357–2363.
29 L. Lin, Y. Liu, L. H. Tang and J. H. Li, *Analyst*, 2011, **22**, 4732–4737.
30 T. Sun, L. Wang, N. Li and X. X. Gan, *Bioprocess Biosyst. Eng.*, 2011, **34**, 1081–1085.
31 Y. P. Wang, Y. H. Xiao, X. L. Ma, N. Li and X. D. Yang, *Chem. Commun.*, 2012, **48**, 738–740.
32 H. Yang, J. Ji, Y. Liu, J. L. Kong and B. H. Liu, *Electrochem. Commun.*, 2009, **11**, 38–40.
33 L. M. Zhu, L. Q. Luo and Z. X. Wang, *Biosens. Bioelectron.*, 2012, **35**, 507–511.
34 Y. Zhang, L. Q. Luo, Y. P. Ding, X. Liu and Z. Y. Qian, *Microchim. Acta*, 2010, **171**, 133–138.
35 Y. Ma, K. Jiao, T. Yang and D. X. Sun, *Sens. Actuators, B*, 2008, **131**, 565–571.
36 Q. X. Wang, B. Zhang, X. Q. Lin and W. Weng, *Sens. Actuators, B*, 2011, **156**, 599–605.
37 C. F. Ding, Y. Ge and J. M. Lin, *Biosens. Bioelectron.*, 2010, **25**, 1290–1294.
38 X. Y. Wang, J. M. Zhou, S. S. Xiao, Z. Chang, P. G. He and Y. Z. Fang, *Anal. Chim. Acta*, 2007, **598**, 242–248.
39 A. Bonanni, A. H. Loo and M. Pumera, *Anal. Chem.*, 2012, **37**, 12–21.
40 M. H. Huang, H. Q. Jiang, X. H. Qu, Z. A. Xu, Y. L. Wang and S. J. Dong, *Chem. Commun.*, 2005, 5560–5562.
41 S. G. Ge, X. L. Jiao and D. R. Chen, *Analyst*, 2012, **137**, 4440–4447.
42 B. L. Hu, R. Quhe, C. Chen, F. Zhuge, X. J. Zhu, S. S. Peng, X. X. Chen, L. Pan, Y. Z. Wu, W. G. Zheng, Q. Yan, J. Lu and R. W. Li, *J. Mater. Chem.*, 2012, **22**, 16422–16430.
43 D. P. Tang, R. Yuan and Y. Q. Chai, *Electroanalysis*, 2006, **18**, 259–266.
44 M. A. Shuman and P. W. Majerus, *J. Clin. Invest.*, 1976, **58**, 1249–1258.
45 Y. Kang, K. J. Feng, J. W. Chen, J. H. Jiang, G. L. Shen and R. Q. Yu, *Bioelectrochemistry*, 2008, **73**, 76–81.
46 F. F. Yan, F. Wang and Z. L. Chen, *Sens. Actuators, B*, 2011, **160**, 1380–1385.
47 Y. Lu, N. N. Zhu, P. Yu and L. Q. Mao, *Analyst*, 2008, **133**, 1256–1260.
48 A. Radi, J. L. A. Sanchez, E. Baldrich and C. K. O'Sullivan, *J. Am. Chem. Soc.*, 2006, **128**, 117–124.
49 L. D. Li, H. T. Zhao, Z. B. Chen, X. J. Mu and L. Guo, *Sens. Actuators, B*, 2011, **157**, 189–194.
50 X. X. Li, L. H. Shen, D. D. Zhang, H. L. Qi, Q. Gao, F. Ma and C. X. Zhang, *Biosens. Bioelectron.*, 2008, **23**, 1624–1630.

